

# Lifetime Prediction of Geogrids for Reinforcement of Embankments and Slopes through Time-Temperature Superposition

† Hyun-Jin Koo, You-Kyum Kim, and Dong-Whan Kim

Reliability Assessment Center, FITI Testing & Research Institute  
892-64 Jegi2-dong, Dongdaemun-gu, Seoul, 130-864, KOREA

The creep resistance of geogrids is one of the most significant long-term safety characteristics used as the reinforcement in slopes and embankments. The failure of geogrids is defined as creep strain greater than 10%. In this study, the accelerated creep tests were applied to polyester geogrids at various loading levels of 30, 50% of the yield strengths and temperatures using newly designed test equipment. Also, the new test equipment permitted the creep testing at or above glass transition temperature( $T_g$ ) of 75, 80, 85°C. The time-dependent creep behaviors were observed at various temperatures and loading levels. And then the creep curves were shifted and superposed in the time axis by applying time-temperature superposition principles. The shifting factors(AFs) were obtained using WLF equation. In predicting the lifetimes of geogrids, the underlying distribution for failure times were determined based on identification of the failure mechanism. The results confirmed that the failure distribution of geogrids followed Weibull distribution with increasing failure rate and the lifetimes of geogrids were close to 100 years which was required service life in the field with 1.75 of reduction factor of safety. Using the newly designed equipment, the creep test of geogrids was found to be highly accelerated. Furthermore, the time-temperature superposition with the newly designed test equipment was shown to be effective in predicting the lifetimes of geogrids with shorter test times and can be applied to the other geosynthetics.

**Keywords:** geogrids, creep, time-temperature superposition, reinforcement, acceleration

## 1. Introduction

The fabric type geogrids are made with a high tenacity polyester filament using a conventional weaving and/or knitting process. Commonly, the fabric type geogrids are then coated with copolymer resins such as PVC(polyvinylchloride), bitumen, PP(polypropylene), acrylic resins, latex and other rubbery materials, which contain a light stabilizer and antioxidant.<sup>1),2)</sup> Since the geogrids possess high tensile properties in nature, they are frequently used as the reinforcement in slopes, embankments, segmental retaining walls and so on<sup>3)</sup> as shown in Fig. 1. The required service lifetime of geogrids used for reinforcement of slopes and embankments varies according to the sensitivity of the environmental condition and required safety factor. Typical lifetimes for slopes and embankments are 50~100 years. This implies that the functional engineering properties of the geogrids should remain within acceptable

limits during the required service life.

Usually, the service lifetime of geogrids are assessed as the long-term creep behavior which causes the shape deformation and collapse of the slopes and embankments. Therefore, various investigators<sup>5),6)</sup> evaluated the time-temperature creep relationship on various geotextiles through accelerated creep testing procedures. Bush<sup>7)</sup> evaluated temperature shifts on geogrids at temperature from 10°C to 40°C. Jeon et. al.<sup>8)</sup> performed the accelerated creep tests on polyester geogrids with various loading levels and temperatures up to 50°C. These studies showed the applicability of predicting creep strains from elevated temperature creep tests. In this study, the long-term creep properties are examined above  $T_g$ (75°C~90°C) by conventional TTS(time-temperature superposition)<sup>4)</sup> using a newly designed test equipment for the first time. The lifetimes of geogrids are predicted through statistical analyses.<sup>9)</sup> It is hoped that via careful interpretation and extrapolation of short-term creep data, accurate long-term creep behavior can be predicted.

† Corresponding author: koojh@fiti.re.kr



Fig. 1. Installation of geogrids

## 2. Theoretical background

### 2.1 Time-temperature superposition

Deformations, such as creep strain, occur relatively rapidly when load first applied, but the rate of increase decreases with time. Consequently, graphs produced with log time as the abscissa are indispensable for describing viscoelastic behavior. The precise way that increasing temperature accelerates these physical processes, governs how creep response can be shifted along a log time scale. The relationship between time and temperature superposition can be explained with the shift factor at the accelerated temperatures. When creep strain is plotted versus time for different temperatures, the creep strain curves along the log of time axis can be shifted until the curves overlap and a single curve is obtained. This curve, the master curve, represents strain for longer time intervals at the reference temperature. The shift factor can be obtained using the WLF equation suggested by William, Landal and Ferry.<sup>4)</sup>

$$E(T_0, t) = E\left(T, \frac{t}{a_T}\right) \quad (1)$$

$$\log a_T = \frac{-C_1(T - T_0)}{(C_2 + T - T_0)} \quad (2)$$

In the WLF equation,  $C_1$  and  $C_2$  vary with material and reference temperature. If the glass transition temperature ( $T_g$ ) is used for extrapolation,  $C_1$  and  $C_2$  take the values 17.4 and 51.6, respectively.

### 2.2 Lifetime prediction

The lifetimes of geogrids are predicted through analyzing the distribution of failure times. A failure distribution represents an attempt to describe mathematically the length

of the life of geogrids. Distinguishing different distribution functions is based on the failure rate known as hazard rate in reliability. Assuming that the geogrids follow an increasing failure rate (IFR) because the failure mode of geogrids is associated with the increase in creep strain due to accumulation of stresses. In order to determine the failure distribution of geogrids, the commonly used failure distribution such as Weibull distribution is as follows,

$$F(t) = 1 - \exp\left[-\left(\frac{t}{\alpha}\right)^\beta\right] \quad (3)$$

$$h(t) = \frac{\beta}{\alpha} \left(\frac{t}{\alpha}\right)^{\beta-1} \quad (4)$$

$$B_{10} = -\alpha [\log(0.9)]^{1/\beta} \quad (5)$$

where,  $\alpha$  is the scale parameter and  $\beta$  is the shape parameter.

In this section, we described the background theories and the practical application of those for lifetime prediction.

## 3. Experimental

### 3.1 Accelerated creep test equipments

The variations in types of polymers and properties of geosynthetics resulted in the development of different creep testing equipment to accommodate the various requirements for clamping mechanisms, specimen's dimensions, temperature ranges, loading levels, testing time, and methods of creep measurement. The accelerated creep test equipment was designed with the following considerations. Fig. 2 shows the newly designed creep test equipment.

The height of loading frame was designed to test upto a 50 cm long geosynthetic specimen. The specimen length was 300 mm long and width was 200 mm wide as in ASTM Test method for Tensile Properties of Geotextiles by the Wide Strip Method D4595.<sup>11)</sup>

A servo motor system that applied the extension loads on the bottom clamps was used in the testing equipment. Such a system offered the flexibility of applying higher loads to each loading frame independently. However, the equipment was costly and required precision and maintenance to keep the applied loads constant within an acceptable range of accuracy during the testing period. The design of the loading system permitted using different clamps according to the types of geosynthetics tested in order to prevent slippage or breakage of the specimens

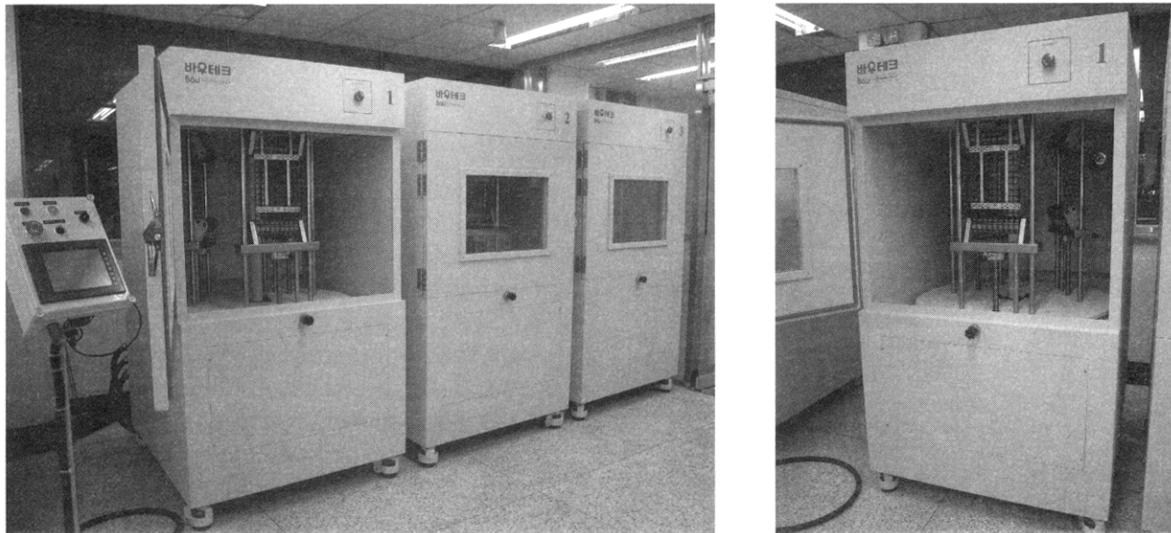


Fig. 2. Accelerated creep test equipment

inside the clamps. Grip type clamps, according to ASTM 4595, were used in testing the geogrids in the creep testing program as shown in Fig. 3.

Creep tests at elevated temperatures were carried out with the geogrid specimens inside temperature-controlled ovens. The ovens were constructed so that 3 sets of loading frames are located inside the ovens which permit the 3 specimens of geogrids tested simultaneously as shown in Fig. 3. The applied load at each frame was monitored using a load cell mounted above the upper clamp. Displacement was monitored by an LVDT (linear variable differential transformer) mounted on the upper plate of the loading frame. The instrument was connected to a data acquisition system and a computer for response monitoring and recording at specific time intervals.

### 3.2 Accelerated creep test

Creep tests were performed on geogrids according to RSK 0008<sup>10)</sup> using a newly designed accelerated creep test equipment with various temperatures and loading levels. Table 1 shows the physical properties of geogrids.

Table 1. Physical properties of polyester geogrids

Physical property		60kN/m designed geogrids
Tensile Strength(kN/m)	Warp	68.2
	Weft	32.1
Elongation(%)	Warp	9.7
	Weft	12.7

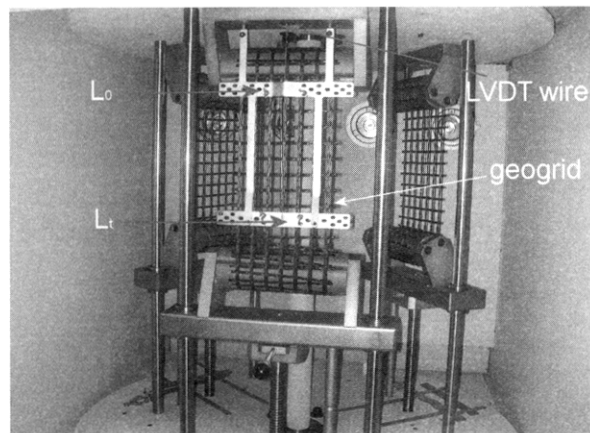
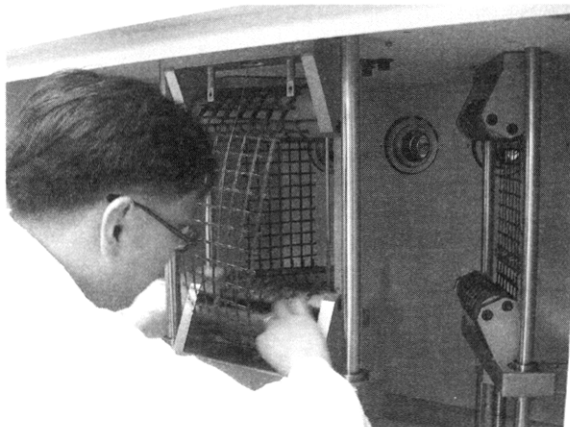
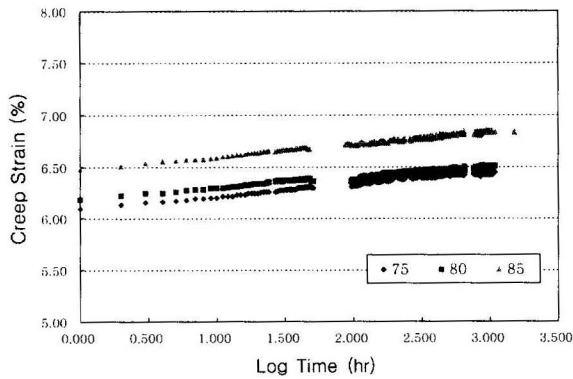


Fig. 3. Loading system and clamping mechanism

Two loading levels were used at 30 and 50% of the yield strength of the geogrids. These tests were performed on three specimens of geogrids at three different levels of temperatures (75, 80 and 85°C) for duration of 1000 h to perform the accelerated tests. The temperature of the oven was maintained by hot air blower within  $\pm 1^\circ\text{C}$  of accuracy.

**4. Results and discussion**

Creep strains for the 60 kN/m geogrids are plotted versus log time at each loading level and temperature as shown in Fig. 4 and 5, respectively. The results show that the creep strain at 50% loading level shows a "typical" plot of strain of geogrids(or its log) versus log time. Initially, the rate of strain increase is high - a wear in period. After a short time, the rate of strain increase becomes relatively constant and remains constant for a considerable time, corresponding to the straight portion of the plot. Finally, the rate of strain increase may increase again - a wear - out period. For, 30% loading level, the wear-out period does not appear.



**Fig. 4.** Creep strain curves of under 30% of yield strength with elevated temperatures

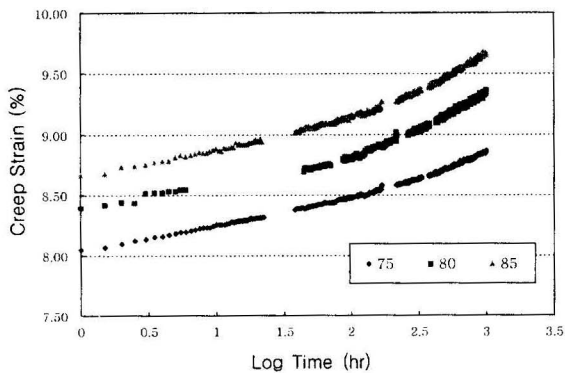


**Fig. 5.** Creep strain curves under 50% of yield strength with elevated temperatures

**4.1 Time-temperature superposition**

The creep strain curves were shifted on the log-time scale to obtain the master curves. Shift factors were calculated based on  $T_g$  as a reference temperature using the Equation 2 as shown in Table 2. The shifting process is illustrated in Fig. 6. The three master curves with the results of linear regression analyses at each loading level were shown in Figs. 7~12. The three master curves show similar shape while the creep strains after TTS are various. The creep strain reaches 6.77~6.83 after TTS for 30% loading level while 9.66~9.95 for 50% loading level. This indicates that the predicted average creep strains are 6.8 and 9.8% for 30 and 50% loading levels after 78 years, respectively.

**Table 2.** Shift factors using WLF equation

Temperature(°C)	Shift factors
75	1
80	-1.54
85	-2.836

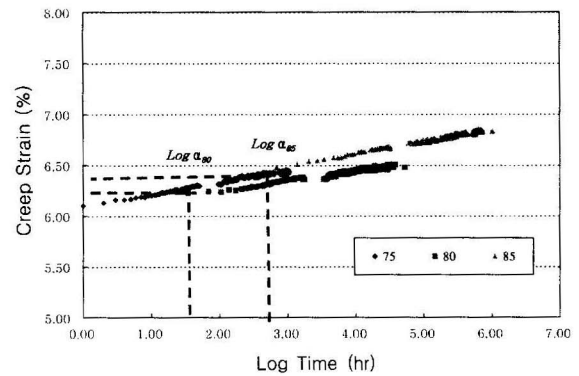


**Fig. 6.** Time-temperature superposition of creep strain curves under 30% of yield strength

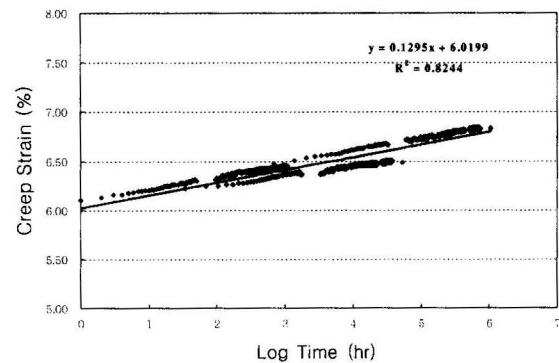


**Fig. 7.** Master curve of specimen 1 under 30% of yield strength

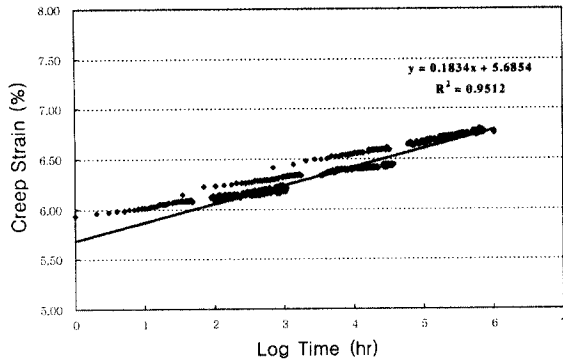


Fig. 8. Master curve of specimen 2 under 30% of yield strength

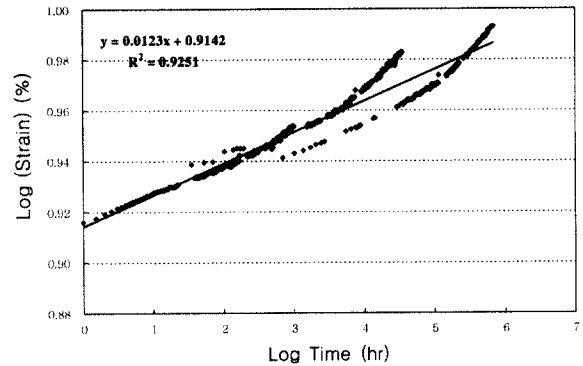


Fig. 11. Master curve of specimen 2 under 50% of yield strength

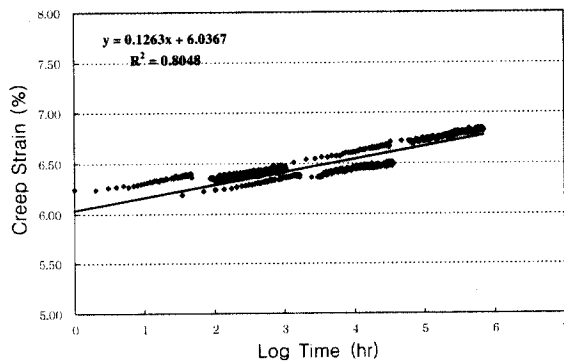


Fig. 9. Master curve of specimen 3 under 30% of yield strength

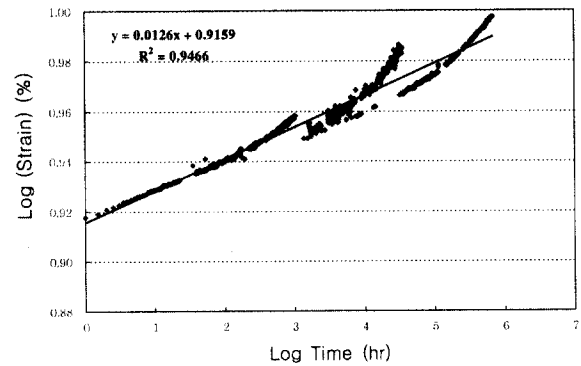


Fig. 12. Master curve of specimen 3 under 50% of yield strength

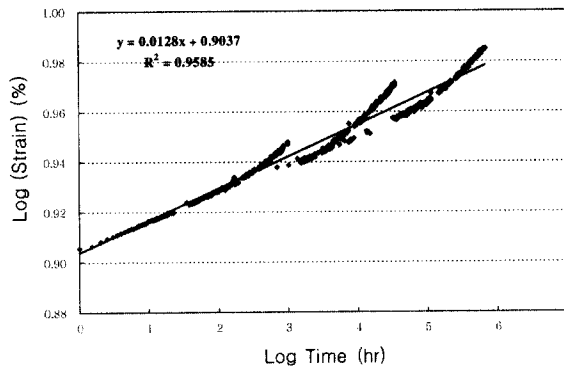


Fig. 10. Master curve of specimen 1 under 50% of yield strength

The linear regression analyses was run for master curves at 50% loading level using the log of creep strain as a response variable for the best fit since those show the "typical" plot. For the master curves at 30% loading level, the log was not taken for creep strain since the plot was almost linear. The master curves with the results of linear regression analyses are given in Fig. 7~12. The estimated failure times of geogrids were extrapolated at 10% creep strain using the linear regression equations. The estimated

failure times are accurate enough for practical usage since  $R^2$  values of regression equations are between 0.80~0.96.

The reduction factor of safety ( $RF$ ) could be calculated from the predicted creep values. The calculated method for that was suggested by R. Koerner<sup>2)</sup> and is presented as follows,

$$RF = \frac{T_{AS}}{T_{DS}} \quad (6)$$

where  $T_{AS}$  is allowable strength of geogrids (10 year design life strength geogrid in sustained tested by ASTM D4595<sup>11)</sup> or sustained ASTM D5262<sup>12)</sup> testing in which the curve becomes asymptotic to a constant strain line, of 10% or less), and  $T_{DS}$  is the design strength of the geogrids. The 50% loading of yield strength means 34 kN/m load applied to geogrids, which is 57%(34/60) of the design strength when the creep strain is asymptotic to 10%. The allowable strength will reflect this type of information in that the partial factor of safety against creep will be the inverse of 57%, which is 1.75.

The failure times ( $FT$ ) were estimated only for 50% loading level as shown in Table 3 since those for 30%

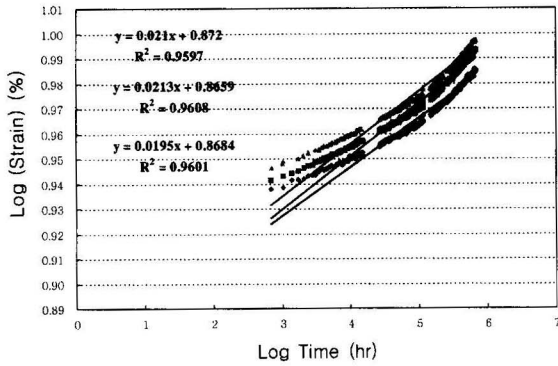


Fig. 13. Regression analysis results and creep strain curves at 85°C under 50% of yield strength

Table 3. Estimated Failure Times at 50% loading level

Specimen	FT(yr)	FT85(yr)
1	533	140
2	1077	227
3	3780	641

loading level are not useful to predict lifetime of geogrids. The reasons for this are in the following. After TTS, the predicted creep strain is close to 10% which reaches a

failure level for 50% loading level. Therefore, the extrapolation using regression equations is possible to estimate the failure times of geogrids. For 30% loading level, it is, however, not practical and useful to estimate the failure times at 10% of creep strain starting from below 7% of actual data in the point of accuracy. Also, the factor of safety with 30% loading level is ineffectively high in the field.

For 50% loading level, we should check another point of view for TTS using WLF shift factors. In this study, we adopt the WLF shift factors instead of empirical ones which can be calculated through experiments with several steps of elevated temperatures. Theoretically, we also can estimate the creep strain after 78 years through accelerated testing during 1000 h at 85°C. The creep strain curves are presented with the equations for linear regression analyses in Fig. 13. The failure times at 10% of creep strain ( $FT_{85}$ ) were estimated using the equations given in Fig. 13 and then shown in Table 3. The lifetimes will be predicted and compared in the following section.

#### 4.2 Lifetime prediction

We predicted the lifetimes of geogrids through estimating failure distributions by applying four different

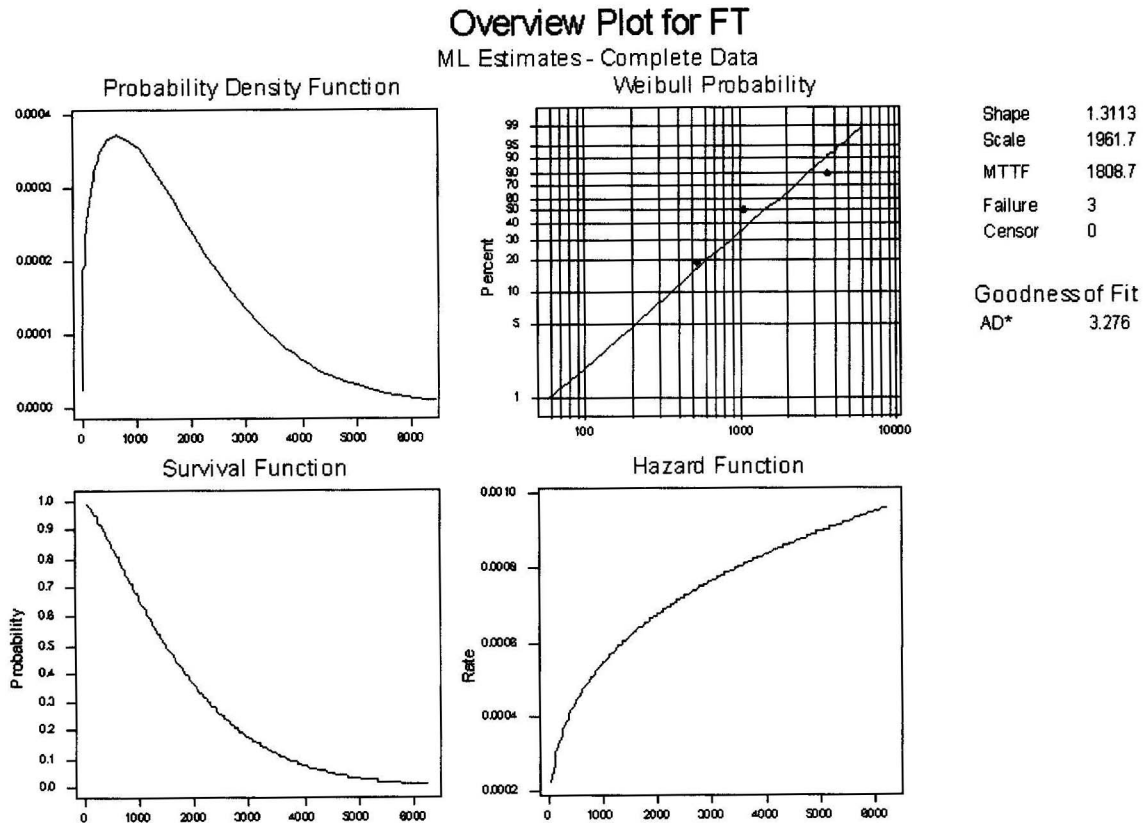


Fig. 14. Results of reliability analyses for FT under 50% of yield strength

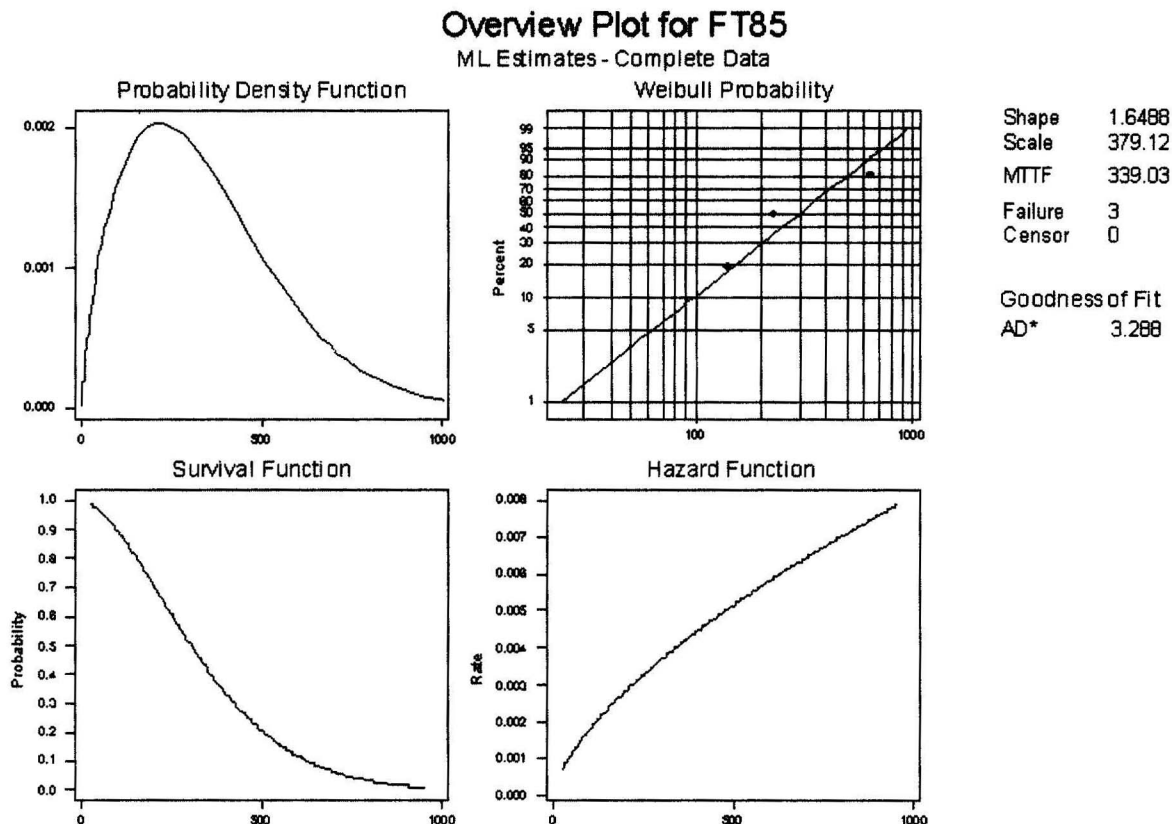


Fig. 15. Results of reliability analyses for FT under 50% of yield strength

statistical distributions to failure times using MINITAB statistical software and test the goodness-of-fit using Anderson-Darling statistics(AD\*).

From the standpoint of reliability considerations, 10 percentile of the distribution with 90% statistical confidence are often of concern. Therefore, we predicted the  $B_{10}$  lifetimes of geogrids. The results show that Weibull distribution fit to failure times for both of  $FT$  and  $FT_{85}$  the best based on Anderson-Darling statistics. This results show that the hazard rate of both cases follow an IFR since the shape parameter for them are slightly greater than 1. The estimated parameters for both distributions are shown in Fig. 14 and 15. The  $B_{10}$  lifetimes of geogrids are 94 years from whole master curves with 90% statistical confidence while those are 34 years from the creep curves

at 85°C as shown in Table 4. This means that the failure data with the whole master curves yield more accurate life estimates than those with creep curves at 85°C even though it is theoretically possible. Therefore, the  $B_{10}$  lifetimes of geogrids satisfy the required service life in the field.

### 5. Conclusions

(1) We have designed new accelerated creep test equipment and a procedure for predicting lifetimes of polyester geogrids by applying statistical failure distributions and time-temperature superposition principles.

(2) The procedure was evaluated for polyester geogrids of an operating temperature above its glass transition temperature(75°C) with two loading levels using the newly designed equipment for the first time. Using this procedure and equipment, the lifetime of geogrids can be predicted longer than 100 years.

(3) The predicted lifetime of geogrids is close to 100 years with 50% loading level equivalent to the reduction factor of 1.75, which is practically and economically acceptable.

Table 4. Results of Lifetime Prediction

Failure time	$B_{10}$ Life(yr) at 50% loading level	90% CI Lower Limit
$FT$ (year)	362	94
$FT_{85}$ (year)	78	34

(4) For more accurate lifetime prediction, the whole master curves are required through time-temperature superposition using creep strain curves at three levels of elevated temperatures.

(5) We also found that the lifetimes of polyester geogrids follow the Weibull distribution and satisfy the required service life used as the reinforcement in slopes and embankments.

(6) The newly designed procedure and equipment could be applied to predict lifetimes of other geosynthetics.

### Acknowledgement

We are grateful to Korean Ministry of Commerce, Industry and Energy for supporting this work.

### References

1. T. S. Ingold, *The geotextiles and geomembranes manual*, Elsevier Advanced Technology, pp.71-246 (1981).
2. R. M. Koerner, *Designing with geosynthetics*, Prentice Hall Co., pp.328-393 (1994).
3. J. A. Finnigan, *The creep behavior of high tenacity yarns and fabrics used in civil engineering applications*, Proceedings of the International Conference on the Use of Fabrics in Geotechnics, Paris, France, pp.645- 650 (1977).
4. J. D. Ferry, *Viscoelastic properties of polymers*, 3<sup>rd</sup> Edition, John Wiley and Sons, NY, USA, (1980).
5. ZK.C. Yeo, *The behavior of polymeric grids used for reinforcement*, Ph. D. thesis, University of Stathelyde, Glasgow, U. K. (1985).
6. J. Muller-Rochholz and R. Kirschner, *Creep of geotextiles at different temperatures*, *Proceedings of 4<sup>th</sup> International Conference on Geotextiles, Geomembranes and Related Products*, The Haque, pp.657-659 (1990).
7. D. I. Bush, *Variation of long term design strength of geosynthetics in temperature up to 40°C*, *Proceedings of 4<sup>th</sup> International Conference on Geotextiles, Geomembranes and Related Products*, The Haque, pp.673-676 (1990).
8. H. Y. Jeon, Seong Hun Kim, and Han Kyu Yoo, *Assessment of long-term performances of polyester geogrids by accelerated creep test*, *Polymer Testing*, **21**, 489 (2002).
9. Wayne Nelson, *Accelerated Testing: Statistical Models, Test Plans, and Data Analyses*, John Wiley and Sons, NY, USA, (1990).
10. RSK 0009, *Geogrids for Reinforcement of embankments and slopes*, (2003).
11. ASTM D4595, *Test method for Tensile Properties of Geotextiles by the Wide Strip Method*, (1986).
12. ASTM D5262, *Standard Test method for Evaluating the Unconfined Tension Creep Behavior of Geosynthetics*, (1997).